,

Modified perfectly matched layer conductivity profile for the alternating direction implicit finite-difference time-domain method with split-field perfectly matched layer

J.-N. Hwang and F.-C. Chen

Abstract: The modified perfectly matched layer (PML) conductivity profiles are proposed to improve the stability of the alternating direction implicit (ADI) finite-difference time-domain (FDTD) method with a split-field PML absorber. The amplification matrix of this scheme is derived based on the Von Neumann method. From the stability analysis, it is found that this scheme is unstable at the PML interface and inside the PML regions. The instability of this scheme inside the PML regions can be improved with the modified PML conductivity profile. The theoretical results are validated by means of numerical simulations.

1 Introduction

The finite-difference time-domain (FDTD) method has been widely used to analyse the electromagnetic problems. Due to its explicit nature, the time step size is restricted by the Courant, Friedrichs and Lewy (CFL) stability condition. Recently, a stable alternating direction implicit (ADI) scheme was introduced for the FDTD method. The ADI-FDTD method is an attractive method because of its unconditional stability with large CFL number [1–3]. To study about unbounded region problems, the split-field perfectly matched layer (PML) [4] was employed for the ADI-FDTD method [5, 6]. However, the implementation of split-field PML in the ADI-FDTD method can affect the stability of this scheme. In [7, 8], from numerical simulation, it is found that the ADI-FDTD method with a split-field PML led to late-time instability. In [7], the authors indicated that the instability from the split-field PML equations can be prevented by using an unsplit form PML implementation. However, the split-field PML formulation is less complicated and more straightforward compared to an unsplit form PML implementation. Therefore a more stable PML implementation for ADI-FDTD method is highly desirable.

In this paper, the theoretical stability analysis of the ADI-FDTD method with split-field PML is described through deriving the amplification matrix. The amplification matrix is derived using the actual updating equations of the field components. From the stability analysis, it is found that this scheme is unstable at the PML interface and inside the PML regions. The effect of the PML conductivity profile on the stability of this scheme is investigated. It is found that the instability of this scheme is due to the conductivities within the PML medium and the instability inside the PML regions can be improved significantly by using a modified PML conductivity profile. Numerical results of the 3-D ADI-FDTD method with split-field PML are demonstrated to validate the theoretical results.

doi:10.1049/iet-map:20060227

Paper first received 5th September 2006 and in revised form 1st May 2007

The authors are with the Department of Communication Engineering, National Chiao Tung University, 1001 Tahsueh Road, Hsinchu 300, Taiwan, Republic of China

E-mail: fchen@faculty.nctu.edu.tw

2 Theoretical amplification matrix

In this section, the amplification matrix of the ADI-FDTD method with split-field PML is derived. For simplicity, a 2-D TM ADI-FDTD is studied. In this scheme, the field components E_{zx}, E_{zy}, H_x and H_y for the first updating procedure can be written as

$$E_{zy\,i,j}^{n+1/2} = C_{ay}E_{zy\,i,j}^{n} - C_{by}\left(H_{xi,j+1/2}^{n} - H_{xi,j-1/2}^{n}\right) \tag{1a}$$

$$\begin{aligned} &E_{zx\,i,j}^{n+1/2}\left(1 + C_{bx}D_{bx,1} + C_{bx}D_{bx,2}\right) \\ &\quad - E_{zx\,i+1,j}^{n+1/2}C_{bx}D_{bx,1} - E_{zx\,i-1,j}^{n+1/2}C_{bx}D_{bx,2} \\ &= C_{ax}E_{zx\,i,j}^{n} + C_{bx} \\ &\quad \times \left(D_{ax,1}H_{y\,i+1/2,j}^{n} - D_{ax,2}H_{y\,i-1/2,j}^{n}\right) \\ &\quad - E_{zy\,i,j}^{n+1/2}\left(C_{bx}D_{bx,1} + C_{bx}D_{bx,2}\right) \\ &\quad + E_{zy\,i+1,j}^{n+1/2}C_{bx}D_{bx,1} + E_{zy\,i-1,j}^{n+1/2}C_{bx}D_{bx,2} \end{aligned} \tag{1b}$$

$$H_{x_{i,j+1/2}}^{n+1/2} = D_{ay,1}H_{x\,i,j+1/2}^{n} - D_{by,1} \times \left(E_{zx\,i,j+1}^{n} + E_{zy\,i,j+1}^{n} - E_{zx\,i,j}^{n} - E_{zy\,i,j}^{n}\right) \tag{1c}$$

$$\begin{aligned} H_{y_{i+1/2,j}}^{n+1/2} &= D_{ax,1}H_{y_{i+1/2,j}}^{n} + D_{bx,1}\left(E_{zx\,i+1,j}^{n+1/2} + E_{zy\,i+1,j}^{n+1/2}\right. \\ &\quad \left. - E_{zx\,i,j}^{n+1/2} - E_{zy\,i,j}^{n+1/2}\right) \end{aligned} \tag{1d}$$

where

$$C_{as} = \frac{1-(\sigma_s \Delta t/4\varepsilon)}{1+(\sigma_s \Delta t/4\varepsilon)} \quad C_{bs} = \frac{\Delta t/2\varepsilon\,\Delta s}{1+(\sigma_s \Delta t/4\varepsilon)}$$

$$D_{as,n} = \frac{1-(\sigma^*_{s,n} \Delta t/4\mu)}{1+(\sigma^*_{s,n} \Delta t/4\mu)} \quad D_{bs,n} = \frac{\Delta t/2\mu\,\Delta s}{1+(\sigma^*_{s,n} \Delta t/4\mu)}$$

$$s = x, y;\ n = 1, 2$$

$$\sigma^*_{x,1} = \sigma^*_{x\,i+1/2,j},\ \sigma^*_{x,2} = \sigma^*_{x\,i-1/2,j},\ \sigma^*_{y,1} = \sigma^*_{y\,i,j+1/2},\ \sigma^*_{y,2} = \sigma^*_{y\,i,j-1/2}$$

Since the electrical conductivity σ and magnetic conductivity σ^* within the PML are usually scaled for small reflection, the PML parameters σ and σ^* in (1) are position dependent. In this study, the amplification matrix is derived using the actual updating equations of field components to capture the effect of the PML conductivity profile.

Similarly, for the second updating procedure, the field components can be written as

$$E^{n+1}_{zx\,i,j} = C_{ax}E^{n+1/2}_{zx\,i,j} + C_{bx}\left(H^{n+1/2}_{y_{i+1/2,j}} - H^{n+1/2}_{y_{i-1/2,j}}\right) \tag{2a}$$

$$\begin{aligned} &E^{n+1}_{zy\,i,j}\left(1 + C_{by}D_{by,1} + C_{by}D_{by,2}\right) \\ &\quad - E^{n+1}_{zy\,i,j+1}C_{by}D_{by,1} - E^{n+1}_{zy\,i,j-1}C_{by}D_{by,2} \\ &= C_{ay}E^{n+1/2}_{zy\,i,j} - C_{by}\left(D_{ay,1}H^{n+1/2}_{x\,i,j+1/2} - D_{ay,2}H^{n+1/2}_{x\,i,j-1/2}\right) \\ &\quad - E^{n+1}_{zx\,i,j}\left(C_{by}D_{by,1} + C_{by}D_{by,2}\right) \\ &\quad + E^{n+1}_{zx\,i,j+1}C_{by}D_{by,1} + E^{n+1}_{zy\,i,j-1}C_{by}D_{by,2} \end{aligned} \tag{2b}$$

$$\begin{aligned} H^{n+1}_{x_{i,j+1/2}} &= D_{ay,1}H^{n+1/2}_{x_{i,j+1/2}} - D_{by,1} \\ &\quad \times \left(E^{n+1}_{zx\,i,j+1} + E^{n+1}_{zy\,i,j+1} - E^{n+1}_{zx\,i,j} - E^{n+1}_{zy\,i,j}\right) \end{aligned} \tag{2c}$$

$$\begin{aligned} H^{n+1}_{y_{i+1/2,j}} &= D_{ax,1}H^{n+1/2}_{y_{i+1/2,j}} + D_{bx,1} \\ &\quad \times \left(E^{n+1/2}_{zx\,i+1,j} + E^{n+1/2}_{zy\,i+1,j} - E^{n+1/2}_{zx\,i,j} - E^{n+1/2}_{zy\,i,j}\right) \end{aligned} \tag{2d}$$

We assume the spatial frequencies to be k_x, k_y and k_z along the x, y and z directions, respectively, and the field components in the spatial spectral domain can be written as

$$E^n_{zx\,i,j} = E^n_{zx}\mathrm{e}^{-j(k_x i\Delta x + k_y j\Delta y)} \tag{3a}$$

$$E^n_{zy\,i,j} = E^n_{zy}\mathrm{e}^{-j(k_x i\Delta x + k_y j\Delta y)} \tag{3b}$$

$$H^n_{x_{i,j+1/2}} = H^n_x\mathrm{e}^{-j(k_x i\Delta x + k_y (j+1/2)\Delta y)} \tag{3c}$$

$$H^n_{y_{i+1/2,j}} = H^n_y\mathrm{e}^{-j(k_x (i+1/2)\Delta x + k_y j\Delta y)} \tag{3d}$$

After substituting these equations into (1), we can obtain

$$\begin{aligned} &E^{n+1/2}_{zx}\left(1 + C_{bx}2jD_{bx,1}\sin\left(\frac{k_x\Delta x}{2}\right)\mathrm{e}^{-j(k_x\Delta x/2)}\right. \\ &\quad \left. - C_{bx}2jD_{bx,2}\sin\left(\frac{k_x\Delta x}{2}\right)\mathrm{e}^{j(k_x\Delta x/2)}\right) \\ &= C_{ax}E^n_{zx} + C_{bx}\left(D_{ax,1}H^n_y\mathrm{e}^{-j(k_x\Delta x/2)} - D_{ax,2}H^n_y\mathrm{e}^{j(k_x\Delta x/2)}\right) \\ &\quad + C_{bx}\left(-2jD_{bx,1}\sin\left(\frac{k_x\Delta x}{2}\right)\mathrm{e}^{-j(k_x\Delta x/2)}\right. \\ &\quad \left. + C_{bx}2jD_{bx,2}\sin\left(\frac{k_x\Delta x}{2}\right)\mathrm{e}^{j(k_x\Delta x/2)}\right)E^{n+1/2}_{zy} \end{aligned} \tag{4a}$$

$$E^{n+1/2}_{zy} = C_{ay}E^n_{zy} + 2jC_{by}\sin\left(\frac{k_y\Delta y}{2}\right)H^n_x \tag{4b}$$

$$H^{n+1/2}_x = D_{ay,1}H^n_x + 2jD_{by,1}\sin\left(\frac{k_y\Delta y}{2}\right)(E^n_{zx} + E^n_{zy}) \tag{4c}$$

$$H^{n+1/2}_y = D_{ax,1}H^n_y - 2jD_{bx,1}\sin\left(\frac{k_x\Delta x}{2}\right)\left(E^{n+1/2}_{zx} + E^{n+1/2}_{zy}\right) \tag{4d}$$

Denote the field vector in the spatial spectral domain as

$$\boldsymbol{X}^n = \left[E^n_{zx} \quad E^n_{zy} \quad H^n_x \quad H^n_y\right]^{\mathrm{T}} \tag{5}$$

The time marching relation of field vector can be written in matrix form as

$$\boldsymbol{M}_1\boldsymbol{X}^{n+(1/2)} = \boldsymbol{P}_1\boldsymbol{X}^n \tag{6}$$

where

$$\boldsymbol{M}_1 = \begin{bmatrix} \begin{pmatrix} 1 + C_{bx}2jD_{bx1}\sin\left(\frac{k_x\Delta x}{2}\right)\mathrm{e}^{-j(k_x\Delta x/2)} \\ -C_{bx}2jD_{bx2}\sin\left(\frac{k_x\Delta x}{2}\right)\mathrm{e}^{j(k_x\Delta x/2)} \end{pmatrix} & 0 & 0 \\ 0 & 0 & 0 \\ 0 & 1 & 0 \\ 2jD_{bx,1}\sin\left(\frac{k_x\Delta x}{2}\right) & 0 & 1 \end{bmatrix}$$

$$\boldsymbol{P}_1 = \begin{bmatrix} C_{ax} & 0 \\ 0 & C_{ay} \\ 2jD_{by,1}\sin\left(\frac{k_y\Delta y}{2}\right) & 2jD_{by,1}\sin\left(\frac{k_y\Delta y}{2}\right) \\ 0 & 0 \end{bmatrix} \times \begin{bmatrix} 0 & C_{bx}\begin{pmatrix} D_{ax1}\mathrm{e}^{-j(k_x\Delta x/2)} \\ -D_{ax2}\mathrm{e}^{j(k_x\Delta x/2)} \end{pmatrix} \\ 2jC_{by}\sin\left(\frac{k_y\Delta y}{2}\right) & 0 \\ D_{ay,1} & 0 \\ 0 & D_{ax,1} \end{bmatrix}$$

We can apply the same procedure for the second updating equations.

$$\boldsymbol{M}_2\boldsymbol{X}^{n+1} = \boldsymbol{P}_2\boldsymbol{X}^{n+(1/2)} \tag{7}$$

where

$$\boldsymbol{M}_2 = \begin{bmatrix} 1 & 0 & 0 & 0 \\ \begin{pmatrix} C_{by}2jD_{by1}\sin\left(\frac{k_y\Delta y}{2}\right)\mathrm{e}^{-j(k_y\Delta y/2)} \\ -C_{by}2jD_{by2}\sin\left(\frac{k_y\Delta y}{2}\right)\mathrm{e}^{j(k_y\Delta y/2)} \end{pmatrix} & \begin{matrix} 0 & 0 \\ 0 & 0 \end{matrix} \\ -2jD_{by,1}\sin\left(\frac{k_y\Delta y}{2}\right) & 1 & 0 \\ 0 & 0 & 1 \end{bmatrix}$$

$$\boldsymbol{P}_2 = \begin{bmatrix} C_{ax} & 0 \\ 0 & C_{ay} \\ 0 & 0 \\ -2jD_{bx,1}\sin\left(\frac{k_x\Delta x}{2}\right) & -2jD_{bx,1}\sin\left(\frac{k_x\Delta x}{2}\right) \end{bmatrix} \begin{bmatrix} 0 & -2jC_{bx}\sin\left(\frac{k_x\Delta x}{2}\right) \\ C_{by}\begin{pmatrix} D_{ay1}\mathrm{e}^{-j(k_y\Delta y/2)} \\ -D_{ay2}\mathrm{e}^{j(k_y\Delta y/2)} \end{pmatrix} & 0 \\ D_{ay,1} & 0 \\ 0 & D_{ax,1} \end{bmatrix}$$

We combine the two half-time steps to one time step

$$\boldsymbol{X}^{n+1} = \boldsymbol{M}_2^{-1}\boldsymbol{P}_2\boldsymbol{M}_1^{-1}\boldsymbol{P}_1\boldsymbol{X}^n = \boldsymbol{\Lambda}\boldsymbol{X}^n \tag{8}$$

It can be found that not only $\sigma^*_{x\,i+1/2,j}$ and $\sigma^*_{y\,i,j+1/2}$ but also $\sigma^*_{x\,i-1/2,j}$ and $\sigma^*_{y\,i,j-1/2}$ are within the amplification matrix $\boldsymbol{\Lambda}$. The stability criterion requires that the eigenvalues of $\boldsymbol{\Lambda}$ lie within or on the unit circle that is $|\lambda_{\boldsymbol{\Lambda}}| \leq 1$

3 Stability analysis

For the stability analysis of this scheme, the eigenvalues of amplification matrix are evaluated. Due to the complexity of the amplification matrix $\boldsymbol{\Lambda}$, it is difficult to obtain the simplified analytical expression for the eigenvalues. The eigenvalues are numerically calculated by Matlab. The stability matrix is a function of a discrete wavenumber. Since the stability must be independent of the angle of wave propagation, all angles must be considered. We find that the maximum eigenvalues occur when $\sin(k_s\Delta s/2) = 1$, where $s = x, y, z$.

A 2-D computation domain that contains 42 × 42 cells is studied. The cell size with $\Delta x = \Delta y = 1.0$ mm and FDTD time step limit $\Delta t_{\max} = 2.35$ ps are used. Ten layers of PML are used in x and y direction. The parameters of PML are chosen the same as those in [5]. A polynomial scaling is used for the PML conductivity profile

$$\sigma_{s\,\max} = \sigma_{\text{opt}} \simeq \frac{(m+1)}{150\pi\Delta s}$$
$$\sigma_s(s) = \frac{\sigma_{s\,\max}|s - s_0|^m}{d^m} \quad s = x, y, z \tag{9}$$

where d is the thickness of PML absorber, Δs is the cell size, and s_0 represents the interface. In this simulation, we choose scaling factor $m = 4$ and $\sigma_{\max} = 10.61$ S/m for optimum PML performance [5].

To validate the proposed amplification matrix, the eigenvalues of amplification matrix are computed for free space condition $\sigma = \sigma^* = 0$ and PML medium with uniform conductivity $\sigma = \sigma_{\max}$. The time step size is $5\Delta t_{\max}$. As shown in Table 1, this scheme is stable under these conditions since all eigenvalues are smaller than unity.

The ADI-FDTD method with the conventional PML conductivity profile (9) is studied. Since the parameters σ and σ^* within the PML are position dependent, the amplification matrix is also different for different PML coefficients. The eigenvalues of amplification matrix are computed for four PML coefficients, as shown in Fig. 1. Position 1 is located at free space. The positions within the PML mediums are studied. Position 2 is located at the interface between the PML and free space where $\sigma^*_{y\,i,j+1/2} = 0$ and $\sigma^*_{y\,i,j-1/2} = 30.1592$. Position 3 is located at the first layer of the PML where $\sigma^*_{y\,i,j+1/2} = 30.1592$ and $\sigma^*_{y\,i,j-1/2} = 934.9371$. Position 4 is located at the eighth layer of PML where $\sigma^*_{y\,i,j+1/2} = 481372.0127$ and $\sigma^*_{y\,i,j-1/2} = 792615.6173$. The condition $\sigma_x = \sigma^*_x = 0$ is used for all the four positions.

The calculated eigenvalues of $\boldsymbol{\Lambda}$ for different time steps and positions are shown in Table 2. For the numerical accuracy, different values are tested to ensure that round-off error does not affect the calculated eigenvalues. As shown in Table 2, it is found that the maximum eigenvalue increases as the time step size increases. This scheme is unstable at Position 2 and Position 3 as the eigenvalues

Table 1: Eigenvalues of Λ for free space and uniform PML mediums σ = σ_max

	Free space $\sigma = 0$	PML medium $\sigma = \sigma_{\max}$
$\lvert\lambda_\Lambda\rvert$	$1.0000000 \times 10^{000}$	$8.7121313 \times 10^{-001}$
	$1.0000000 \times 10^{000}$	$8.7121313 \times 10^{-001}$
	$1.0000000 \times 10^{000}$	$4.8417857 \times 10^{-001}$
	$1.0000000 \times 10^{000}$	$4.8417857 \times 10^{-001}$

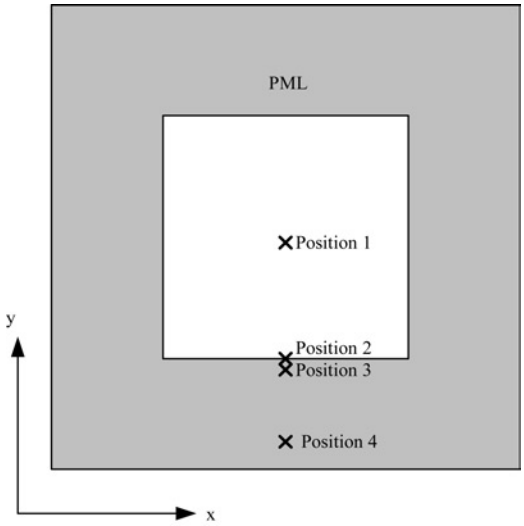

Fig. 1 *Four positions for eigenvalue calculation*

are larger than unity. In [7], it has been described that the instability of the ADI-FDTD method with split-field PML was unavoidable. The eigenvalue of this scheme with time step size less than the CFL limit is also investigated. It can be seen that some eigenvalues are larger than unity at Position 2 and Position 3 when the time step size $0.9\Delta t_{\max}$ is used.

4 Modified conductivity profiles

The PML conductivity profile affects the stability of the ADI-FDTD method when a split-field PML is used. As shown in Table 2, it is found that all the eigenvalues are smaller than unity at Position 4. We find that there are two conditions for this scheme to be stable inside the PML regions. The first condition is that the ratio of the successive magnetic conductivities in the PML should be small and the second condition is that the electrical and magnetic conductivities inside the PML regions should be large enough. Since the PML conductivity is increased from the PML interface to the PEC boundary, it is found that the ratio of the successive magnetic conductivities in the PML close to the PML interface should be smaller than 1.3 and that close to the PEC boundary should be smaller than 1.5 to avoid the instability.

The effect of the conductivity profile on the stability of this scheme is investigated. Two modified conductivity profiles are studied. For the first modified conductivity profile, the $\sigma_{\max} = 10.61$ S/m and the ratio of the successive magnetic conductivities inside the PML regions are arranged as

$$\frac{\sigma^*_{x,2}}{\sigma^*_{x,1}} = \frac{\sigma^*_{y,2}}{\sigma^*_{y,1}} = 1.3 \text{ (from 1st layer to 3rd layer)}$$

$$\frac{\sigma^*_{x,2}}{\sigma^*_{x,1}} = \frac{\sigma^*_{y,2}}{\sigma^*_{y,1}} = 1.4 \text{ (from 4th layer to 5th layer)}$$

$$\frac{\sigma^*_{x,2}}{\sigma^*_{x,1}} = \frac{\sigma^*_{y,2}}{\sigma^*_{y,1}} = 1.5 \text{ (from 6th layer to 10th layer)} \quad (10)$$

The increase of the PML conductivity of (10) is not polynomially scaled. Therefore the PML performance with the first modified PML conductivity profile (10) is significantly affected. A second modified PML conductivity profile with a constant scaling factor m is proposed. In this modified PML conductivity profile, the successive PML conductivity is scaled using the polynomial function (9) with $\sigma_{\max} = 21.22$ S/m and $m = 2$.

$$\sigma_s(s) = \frac{\sigma_{s\max}|s - s_0|^2}{d^2} \quad s = x, y, z \quad (11)$$

The corresponding normal reflection coefficient $R(0)$ of (11) is 6.8×10^{-24}, which is much smaller than the conventional value. The comparisons between the conventional PML conductivity profile (9), the first modified conductivity profile (10) and the second modified conductivity profile (11) are shown in Fig. 2.

The same 2-D computation domain is studied. The time step is $5\Delta t_{\max}$. The calculated eigenvalues of this scheme with different conductivity profiles at different positions are shown in Table 3. First, the PML medium with a uniform conductivity $\sigma = 10.61$ is studied. It is found that this scheme can be stable inside the PML regions. However, the maximum eigenvalue at the (21, 10) is larger than unity. The instability of this scheme at the

Table 2: Eigenvalues of Λ for 2-D ADI-FDTD with PML

	Position 1 (21, 20)	Position 2 (21, 10)	Position 3 (21, 9)	Position 4 (21, 2)
$00.9\Delta t_{\max}$	$1.0000000 \times 10^{000}$	$9.9999985 \times 10^{-001}$	$9.9991584 \times 10^{-001}$	$6.9932975 \times 10^{-001}$
	$1.0000000 \times 10^{000}$	$9.9999985 \times 10^{-001}$	$9.9991584 \times 10^{-001}$	$6.9932975 \times 10^{-001}$
	$1.0000000 \times 10^{000}$	$1.0000000 \times 10^{000}$	$9.9977724 \times 10^{-001}$	$6.4315304 \times 10^{-001}$
	$1.0000000 \times 10^{000}$	$1.0000021 \times 10^{000}$	$1.0000735 \times 10^{000}$	$6.4315304 \times 10^{-001}$
$\Delta t_{\max}$	$1.0000000 \times 10^{000}$	$9.9999977 \times 10^{-001}$	$9.9990957 \times 10^{-001}$	$6.8325119 \times 10^{-001}$
	$1.0000000 \times 10^{000}$	$9.9999977 \times 10^{-001}$	$9.9990957 \times 10^{-001}$	$6.8325119 \times 10^{-001}$
	$1.0000000 \times 10^{000}$	$1.0000000 \times 10^{000}$	$9.9974524 \times 10^{-001}$	$6.1599183 \times 10^{-001}$
	$1.0000000 \times 10^{000}$	$1.0000028 \times 10^{000}$	$1.0001031 \times 10^{000}$	$6.1599183 \times 10^{-001}$
$2\Delta t_{\max}$	$1.0000000 \times 10^{000}$	$9.9999766 \times 10^{-001}$	$9.9983507 \times 10^{-001}$	$5.8437802 \times 10^{-001}$
	$1.0000000 \times 10^{000}$	$9.9999766 \times 10^{-001}$	$9.9983507 \times 10^{-001}$	$5.8437802 \times 10^{-001}$
	$1.0000000 \times 10^{000}$	$1.0000000 \times 10^{000}$	$9.9940408 \times 10^{-001}$	$3.9758804 \times 10^{-001}$
	$1.0000000 \times 10^{000}$	$1.0000141 \times 10^{000}$	$1.0005628 \times 10^{000}$	$3.9758804 \times 10^{-001}$
$4\Delta t_{\max}$	$1.0000000 \times 10^{000}$	$9.9998999 \times 10^{-001}$	$9.9960137 \times 10^{-001}$	$7.2137644 \times 10^{-001}$
	$1.0000000 \times 10^{000}$	$9.9998999 \times 10^{-001}$	$9.9960137 \times 10^{-001}$	$5.0510375 \times 10^{-001}$
	$1.0000000 \times 10^{000}$	$1.0000000 \times 10^{000}$	$9.9871437 \times 10^{-001}$	$5.0510375 \times 10^{-001}$
	$1.0000000 \times 10^{000}$	$1.0000451 \times 10^{000}$	$1.0017621 \times 10^{000}$	$1.5426083 \times 10^{-002}$

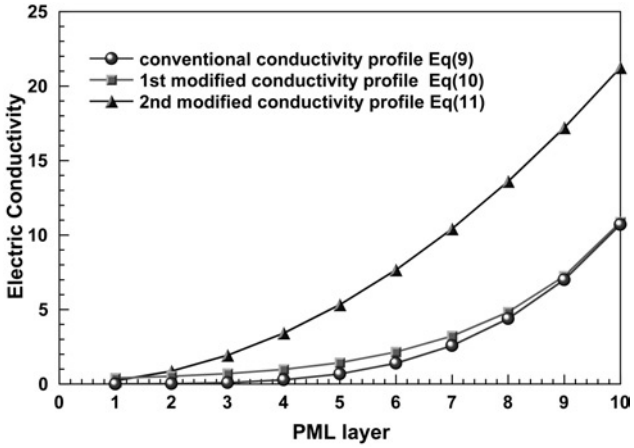

Fig. 2 *Conductivity profiles for the PML mediums*

PML interface is unavoidable. Although the instability inside the PML regions can be improved, this scheme suffers from larger reflection errors since the conductivity is not increased from the PML interface to the PEC boundary. The conventional conductivity profile (9) for optimum PML performance is studied. As shown in Table 3, this scheme is unstable from position (21, 10) to position (21, 3) and is stable from position (21, 2) with the conventional conductivity profile. This is because the ratio of the successive magnetic conductivities in the PML layers is less than 1.5 only at the regions close to the PEC boundary.

The ADI-FDTD method with the modified PML conductivity profile is studied. For the first modified conductivity profile (10), it is found that all the eigenvalues of this scheme are smaller than unity from position (21, 9) to position (21, 1), which means this scheme is stable inside the PML region. For the second modified conductivity profile (11), the ratio of the successive magnetic conductivities in

Table 3: Calculated eigenvalues of Λ for different conductivity profiles

	Position (21, 10)	Position (21, 9)	Position (21, 8)	Position (21, 7)	Position (21, 6)	Position (21, 3)	Position (21, 2)
Uniform PML medium $\sigma = 10.61$	8.3167465 $\times 10^{-001}$	8.7121313 $\times 10^{-001}$	8.7121313 $\times 10^{-001}$	8.7121313 $\times 10^{-001}$	8.7121313 $\times 10^{-001}$	8.7121313 $\times 10^{-001}$	8.7121313 $\times 10^{-001}$
	8.3167465 $\times 10^{-001}$	8.7121313 $\times 10^{-001}$	8.7121313 $\times 10^{-001}$	8.7121313 $\times 10^{-001}$	8.7121313 $\times 10^{-001}$	8.7121313 $\times 10^{-001}$	8.7121313 $\times 10^{-001}$
	1.0000000 $\times 10^{00}$	4.8417857 $\times 10^{-001}$	4.8417857 $\times 10^{-001}$	4.8417857 $\times 10^{-001}$	4.8417857 $\times 10^{-001}$	4.8417857 $\times 10^{-001}$	4.8417857 $\times 10^{-001}$
	2.2607177 $\times 10^{00}$	4.8417857 $\times 10^{-001}$	4.8417857 $\times 10^{-001}$	4.8417857 $\times 10^{-001}$	4.8417857 $\times 10^{-001}$	4.8417857 $\times 10^{-001}$	4.8417857 $\times 10^{-001}$
Conventional conductivity profile	9.9998595 $\times 10^{-001}$	9.9947387 $\times 10^{-001}$	9.9501294 $\times 10^{-001}$	9.7672831 $\times 10^{-001}$	9.2963950 $\times 10^{-001}$	8.0873543 $\times 10^{-001}$	8.5231622 $\times 10^{-001}$
	9.9998595 $\times 10^{-001}$	9.9947387 $\times 10^{-001}$	9.9501294 $\times 10^{-001}$	9.7672831 $\times 10^{-001}$	9.2963950 $\times 10^{-001}$	3.4158314 $\times 10^{-001}$	5.8450767 $\times 10^{-001}$
	1.0000607 $\times 10^{00}$	1.0023617 $\times 10^{000}$	9.8273693 $\times 10^{-001}$	9.2571923 $\times 10^{-001}$	7.9713001 $\times 10^{-001}$	5.3701283 $\times 10^{-002}$	5.1407068 $\times 10^{-001}$
	1.0000000 $\times 10^{00}$	9.9837472 $\times 10^{-001}$	1.0149820 $\times 10^{000}$	1.0462747 $\times 10^{000}$	1.0958000 $\times 10^{00}$	1.0400832 $\times 10^{00}$	3.3159060 $\times 10^{-002}$
First modified conductivity profile	9.7912834 $\times 10^{-001}$	8.8457772 $\times 10^{-001}$	8.5285313 $\times 10^{-001}$	8.4633346 $\times 10^{-001}$	8.8028977 $\times 10^{-001}$	7.7235998 $\times 10^{-001}$	5.7646377 $\times 10^{-001}$
	9.7912834 $\times 10^{-001}$	8.8457772 $\times 10^{-001}$	8.5285313 $\times 10^{-001}$	7.7764778 $\times 10^{-001}$	6.3334230 $\times 10^{-001}$	8.6715348 $\times 10^{-001}$	5.7646377 $\times 10^{-001}$
	1.0952721 $\times 10^{00}$	7.6986223 $\times 10^{-001}$	7.1107860 $\times 10^{-001}$	6.1748176 $\times 10^{-001}$	5.0285471 $\times 10^{-001}$	2.5298972 $\times 10^{-001}$	7.4761908 $\times 10^{-001}$
	1.0000000 $\times 10^{00}$	9.8777229 $\times 10^{-001}$	9.8155369 $\times 10^{-001}$	9.9755841 $\times 10^{-001}$	9.8509416 $\times 10^{-001}$	1.2658093 $\times 10^{-002}$	8.5740395 $\times 10^{-002}$
Second modified conductivity profile	9.9540604 $\times 10^{-001}$	9.5110019 $\times 10^{-001}$	8.1956499 $\times 10^{-001}$	8.3465030 $\times 10^{-001}$	9.2765962 $\times 10^{-001}$	8.4492806 $\times 10^{-001}$	9.0538676 $\times 10^{-001}$
	9.9540604 $\times 10^{-001}$	9.5110019 $\times 10^{-001}$	8.1956499 $\times 10^{-001}$	4.6990210 $\times 10^{-001}$	7.5040601 $\times 10^{-001}$	8.4492806 $\times 10^{-001}$	9.0538676 $\times 10^{-001}$
	1.0200902 $\times 10^{00}$	8.1340254 $\times 10^{-001}$	4.9000128 $\times 10^{-001}$	1.7718996 $\times 10^{-001}$	3.0547466 $\times 10^{-001}$	4.7954231 $\times 10^{-001}$	5.2417697 $\times 10^{-001}$
	1.0000000 $\times 10^{00}$	1.1607705 $\times 10^{000}$	1.2344384 $\times 10^{000}$	1.1379080 $\times 10^{000}$	1.7064586 $\times 10^{-002}$	4.7954231 $\times 10^{-001}$	5.2417697 $\times 10^{-001}$

the PML is smaller than 1.5 from position (21, 6) to position (21, 1). As shown in Table 3, the calculated eigenvalues of this scheme with the second modified conductivity profile is stable in these positions. Compared to the conventional conductivity profile, the instability inside the PML region can also be improved significantly with the second modified conductivity profile.

The PML performances of this scheme with the modified conductivity profiles are studied. A differentiated Gaussian pulse is launched for the H component. The source excitation is located at (21, 21) and the observation position is located ten cells away from the excitation and close to the PML interface. The relative reflection error of the PML is evaluated by

$$R = 20\log_{10}\left(\frac{|H^{\mathrm{t}} - H^{\mathrm{t}}_{\mathrm{ref}}|}{\max|H^{\mathrm{t}}_{\mathrm{ref}}|}\right) \tag{12}$$

where H^{t} is the H field component recorded at the observation point and $H^{\mathrm{t}}_{\mathrm{ref}}$ is the reference value calculated from a large enough domain. The recorded H components for TM and TE waves are H_x and H_z fields, respectively. The calculated relative reflection errors of the 2-D TM and TE waves are shown in Fig. 3*a* and 3*b*, respectively. In the PML equations, σ^*_y is used in the H_y equation and both the σ^*_x and σ^*_y are used in the H_{zx} and H_{zy} equations, respectively. Therefore the calculated reflection errors of TM and TE waves are somewhat different. As shown in Fig. 3*a* and 3*b*, the results are compared to the PML scheme with the conventional PML conductivity profile. For the first modified PML conductivity profile (10), it is found that the PML performance deteriorates at about 22 and 16 dB for TM and TE waves, respectively. For the second modified conductivity profile (11), the maximum reflection error is reduced to 12 and 1.8 dB for TM and TE waves, respectively. The PML performance of the ADI-FDTD with the second modified PML conductivity profile is better than with that of the first modified PML conductivity profile, as shown in Fig. 3. Although the PML performance of first modified PML conductivity profile can be improved by increasing the PML thickness, the corresponding conductivity becomes small and the instability of this scheme also increases. From Table 3, it is found that the ADI-FDTD scheme with the first modified PML conductivity profile is unstable in the vacuum–PML regions. The worse PML performance of the first modified PML conductivity profile makes this scheme more unstable since the reflection wave from the boundary is amplified in the unstable vacuum–PML regions.

As shown in Table 3, the instability of the ADI-FDTD with PML can also be improved if the second modified PML conductivity profile is employed and the PML performance can still be maintained. The first modified conductivity can be viewed as a guideline for the design of the stable split-field PML. By considering the PML performance and the stability of this scheme, the second modified PML profile (11) is more suitable for the ADI-FDTD simulation.

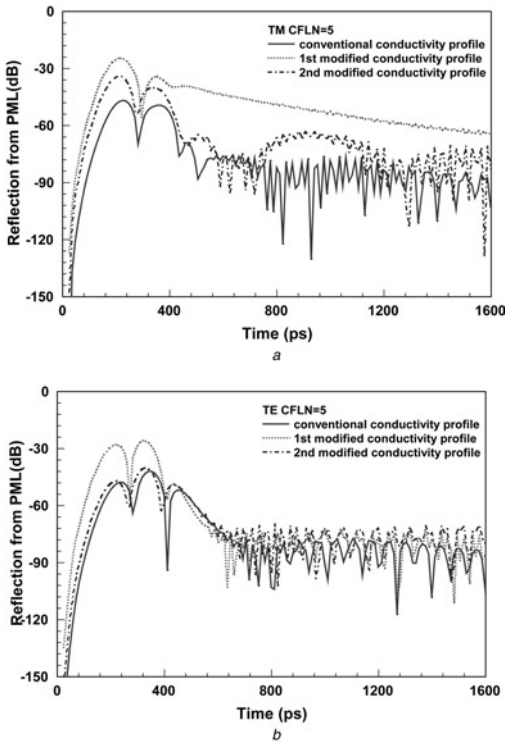

Fig. 3 *Calculated relative reflection error of the 2-D TM and TE wave*

a Relative reflection error of the 2-D TM ADI-FDTD method with PML ABC

b Relative reflection error of the 2-D TE ADI-FDTD method with PML ABC

5 Numerical simulation

In Section 2, the theoretical amplification matrix is derived based on the Von Neumann method. The Von Neumann method assumes that the wave propagates in an unbounded region. If the calculated eigenvalues of ADI-FDTD with split-field PML are larger than unity, it means that the electromagnetic field is unstable in the homogenous region with these PML coefficients. Since the ADI scheme is unstable with these PML coefficients, the ADI-FDTD with PML implementation would also become unstable. A method to validate the instability of the ADI-FDTD with PML implementation is to calculate the amplification matrix of the total computational domain. However, the amplification matrix of the total computational domain is very complicated and is not suitable for other problems. A simple way to analyse the stability of the total computational domain can be accomplished by numerical simulations. In this section, the numerical tests of the ADI-FDTD method with split-field PML are performed. From the stability analysis, it is found that the ADI-FDTD method with split-field PML is unstable at the vacuum–PML interface and inside the PML regions. For a 2-D case, the eigenvalue is small and it requires a large number of time steps to make the field components unstable. Numerical simulation is

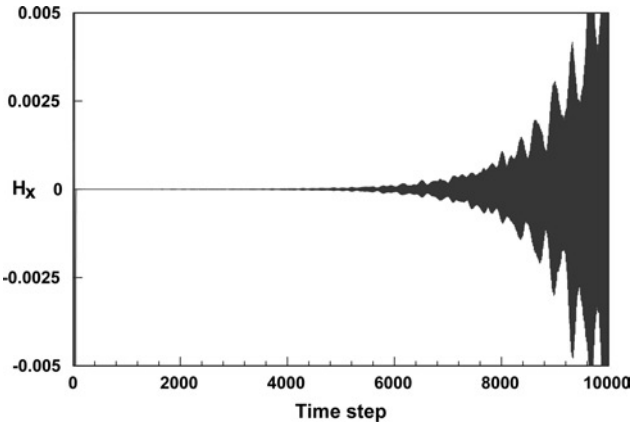

Fig. 4 *H_x component with the conventional conductivity profile*

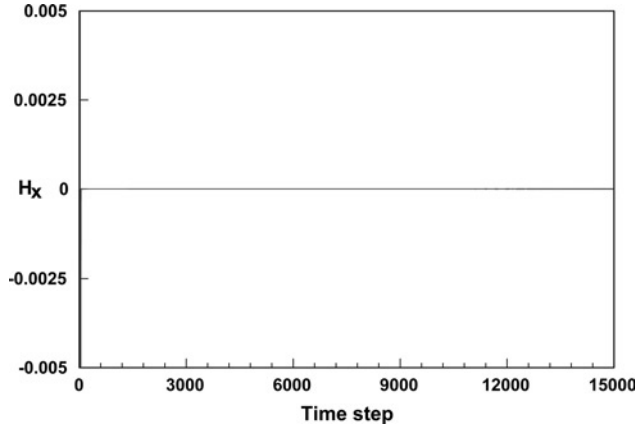

Fig. 5 *H_x component with the modified PML conductivity profile*

performed for a 3-D ADI-FDTD method with split-field PML. A uniform mesh with cell size $\Delta x = \Delta y = \Delta z = 1.0$ mm and FDTD time step limit $\Delta t_{\max} = 1.92$ ps are used. The computation domain is $42 \times 42 \times 42$. PML layers that are ten cells thick terminated all six sides of the computation domain. A differential Gaussian pulse applied to H_x field is excited at the centre position (21, 21, 21) and the time step size in this study is $5\Delta t_{\max}$. First, the numerical simulation of this scheme with the conventional PML conductivity profile (9) is performed. Fig. 4 shows the time-domain H_x fields recorded at the position (21, 20, 21). As shown in Fig. 4, this scheme becomes unstable after running 3500 time steps.

After considering the PML performance, this scheme with the second modified PML conductivity profile (11) is studied. Fig. 5 shows the simulated time-domain H_x fields. No instability is observed after running 15 000 time steps. Although there are several eigenvalues larger than unity and the PML performance is affected by the second modified conductivity profile, it is found that the stability of this scheme can be significantly improved.

6 Conclusion

In this work, the stability analysis of the ADI-FDTD method with split-field PML mediums is studied. It is found that this scheme is unstable at the vacuum–PML interface and inside the PML regions. The instability of this scheme inside the PML regions can be improved by using the modified conductivity profile. The theoretical results are validated by numerical simulations.

7 References

1 Namiki, T.: 'A new FDTD algorithm based on alternating-direction implicit method', *IEEE Trans. Microw. Theory Tech.*, 1999, **47**, (10), pp. 2003–2007

2 Zheng, F., Chen, Z., and Zhang, J.: 'A finite-difference time-domain method without Courant stability conditions', *IEEE Microw. Guid. Wave Lett.*, 1999, **9**, (11), pp. 441–443

3 Zheng, F., Chen, Z., and Zhang, J.: 'Toward the development of a three-dimensional unconditionally stable finite-difference time-domain method', *IEEE Trans. Microw. Theory Tech.*, 2000, **48**, (9), pp. 1550–1558

4 Berenger, J.P.: 'A perfectly matched layer for the absorbing of electromagnetic waves', *J. Comp. Phys.*, 1994, **114**, pp. 185–200

5 Liu, G., and Gedney, S.D.: 'Perfectly matched layer media for an unconditionally stable three-dimensional ADI-FDTD method', *IEEE Microw. Guid. Wave Lett.*, 2000, **10**, (7), pp. 261–263

6 Chen, C.C.-P., Lee, T.-W., Murugensan, N., and Hagness, S.C.: 'Generalized FDTD-ADI: an unconditionally stable full-wave Maxwell's equations solver for VLSI interconnect modeling'. Proc. Int. Conf. on Computer-Aided Design, San Jose, CA, November 2000, pp. 156–163

7 Rubio, R.G., Garcia, S.G., Bretones, A.R., and Martin, R.G.: 'An unsplit Berenger-like PML for the ADI-FDTD method', *Microw. Opt. Technol. Lett.*, 2004, **42**, (6), pp. 466–469

8 Hwang, J.-N., and Chen, F.-C.: 'A rigorous stability analysis of instability in ADI-FDTD method with PML absorber'. IEEE AP-S Int. Symp. Digest, July 2006, pp. 1739–1742